



ELSEVIER

Contents lists available at ScienceDirect

## Journal of Magnetism and Magnetic Materials

journal homepage: [www.elsevier.com/locate/jmmm](http://www.elsevier.com/locate/jmmm)

## Research articles

## Electric field control for energy efficient domain wall injection

F.N. Tan<sup>a,b</sup>, Q.Y. Wong<sup>a,b</sup>, W.L. Gan<sup>a</sup>, S.H. Li<sup>a</sup>, H.X. Liu<sup>b</sup>, F. Poh<sup>b</sup>, W.S. Lew<sup>a,\*</sup><sup>a</sup> School of Physical and Mathematical Sciences, Nanyang Technological University, 21 Nanyang Link, Singapore 637371, Singapore<sup>b</sup> GLOBALFOUNDRIES Singapore Pte, Ltd., 738406, Singapore

## A B S T R A C T

Domain wall injection by electric means is an energy exhausting process. This process is conventionally carried out by sending a current pulse through a stripline which generates an Oersted field to locally switch the magnetization in a magnetic wire. In this work, the magnetic properties of the device were modulated by electric control to lower the required current density for DW injection. The proposed DW injection device employs a Hall cross structure which simplifies the device fabrication process and allows a larger Oersted field to be generated at the domain wall injection region. Electrical pulses of 50 ns were sent through the Hall bar to inject domain walls. The formation of the resulting domain walls was detected electrically using the Hall resistance and optically by Kerr microscopy. The results show that the required current density for injection of domain walls is reduced by  $\sim 20\%$  with an applied electric field of +250 MV/m on the Hall cross structure.

Domain wall (DW) based memory device has garnered research interest for many years due to its potential as a universal memory device [1–4]. Unlike a hard disk drive, these non-volatile memory devices operate without the use of any mechanical part. In conjunction with thermally robust magnetic materials, this ensures the reliability of the device for many decades. In any DW based memory device, write operation of the device involves the propagation of the domain wall and the injection of domain walls. The domain wall injection process consumes the largest amount of energy due to the need for magnetization switching. The amount of energy required to inject DWs in a magnetic wire with perpendicular magnetic anisotropy (PMA) can be estimated with  $K_{anis} \cdot V$ , where  $K_{anis}$  refers to the magnetic anisotropy energy and  $V$  represents the magnetic volume [5]. Therefore, a magnetic thin film with low  $K_{anis}$  is desired for energy efficient domain wall injection. However, the material requires a high  $K_{anis}$  for thermal stability [6–8]. The thermal stability can be represented with  $K_{anis}V/k_B T$ , where  $k_B$  and  $T$  represents the Boltzmann constant and temperature respectively. Therefore, a high  $K_{anis}$  is desirable for magnetic memory devices for thermal robustness, but a low  $K_{anis}$  can lower the energy requirement of DW injection. This dilemma can be resolved if electric field control is used to lower the  $K_{anis}$  of the device only when DW injection is required. Conventionally, the DW injection is achieved by applying an electrical current into a conductive stripline fabricated orthogonally to the magnetic wire. The applied current generates an Oersted field which switches the local magnetization of the magnetic wire around the region under the stripline [9–12]. This DW injection technique has enabled a multitude of studies on DW based devices including logic operations [13] and the study of DW propagation [14–16] and DW pinning [10,17].

Despite DW injection being the most energy exhaustive process in any DW based memory device, the energy efficiency of DW injection using Oersted field has been relatively unexplored. In this work, DW injection is achieved by applying an electrical current pulse through a Hall cross structure. The  $K_{anis}$  of the device is modulated by electric field control, which allows DWs to be injected with a lower current density. The experimental results obtained from a custom-built Kerr microscopy setup [18,19] were substantiated by Hall resistance measurement to show that the electric field modulation is able to reduce the required current density for injection of DWs.

Electric field control requires an insulating interface on the magnetic wire, which is usually achieved by oxide deposition on top of the magnetic wire [20–27]. However, the conductive stripline which generates the Oersted field is also conventionally deposited on top of the magnetic wire [9–12]. The simple solution would be to shift either the stripline or the insulating layer below the magnetic nanowire. However, this would involve complicated fabrication processes to ensure flatness before the deposition of the magnetic film. An uneven surface can give rise to pinning or nucleation sites around the domain injection region which might lead to false positive readings. Therefore, a Hall cross structure was employed as a DW injection device, where the Hall bar serves as the conductive stripline for Oersted field generation. The fabrication processes for the Hall cross device is simpler, and also allows the magnetic thin film to be deposited onto a flat, homogenous surface.

A combination of electron beam lithography, ion milling and lift-off techniques were used to fabricate the Hall cross device. To apply an electric field onto the Hall cross device,  $\text{HfO}_x$  was chosen to be the insulator as it has a high- $\kappa$  value, and ITO was employed to be the gate

\* Corresponding author.

E-mail address: [wensiang@ntu.edu.sg](mailto:wensiang@ntu.edu.sg) (W.S. Lew).<https://doi.org/10.1016/j.jmmm.2019.04.069>

Received 20 December 2018; Received in revised form 17 March 2019; Accepted 16 April 2019

Available online 19 April 2019

0304-8853/© 2019 Elsevier B.V. All rights reserved.

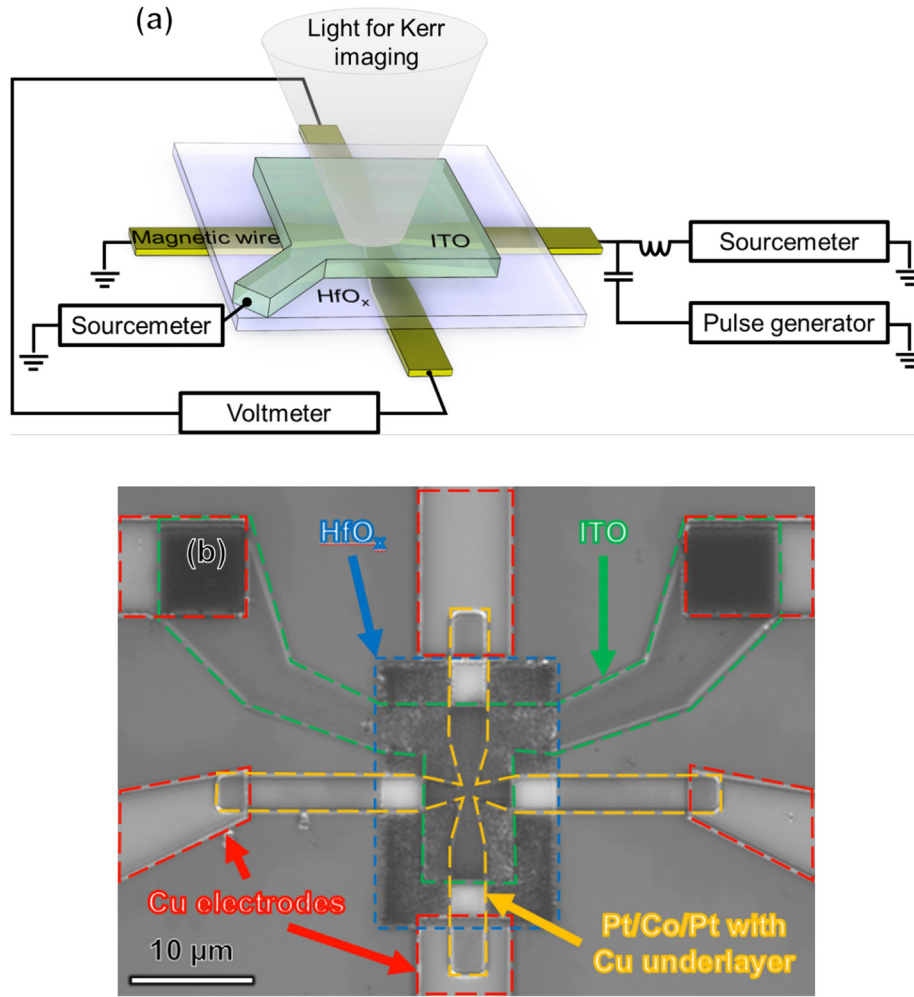


**Fig. 1.** (a) Schematic diagram illustrating the DW injection observed using Kerr imaging and electric measurement. (b) Microscope image of Hall cross device. The white regions are caused by the thin-film interference of the HfO<sub>x</sub>.

electrode due to it being transparent and electrically conductive. Fig. 1(a) shows a schematic diagram of the fabricated Hall cross structure under Kerr imaging and electric measurement. Fig. 1(b) shows the microscope image of the Hall cross structure designed for DW injection. In order for sufficient current to pass through the Hall bar to generate significant Oersted field, a [Cu/ Ta]<sub>4</sub> stack was deposited below the magnetic Co layer to increase conductivity. The resulting stack used to fabricate the Hall cross device is Ta(3)/[Cu (25)/Ta (1)]<sub>4</sub>/Pt (3)/Co (1)/Pt (0.4), where the numbers in parentheses represents the thickness in nanometres. Vibrating sample magnetometry of various deposited thin films with and without the conductive Cu layers is shown in Fig. S1 from the supplementary material. The conductive Cu layer under the magnetic layer does not affect the magnetic properties of the thin film. The materials in this work were deposited by magnetron sputtering with a base pressure of  $5 \times 10^{-8}$  Torr or lower.

The Hall cross device proposed in this work for use as a DW injection device has a geometrical constriction as shown in Fig. 1(b). This was designed to increase the current density and Oersted field at the injection region. Simulations performed with COMSOL Multiphysics show that the current density is larger at the corners of all the Hall cross structures, thereby giving rise to a larger Oersted field at the corners ( $H_0$ ). A comparison of the proposed structure with two conventional Hall cross structures of different widths is shown in Fig. 2. The left and centre of Fig. 2 show a conventional Hall cross device with a width of 3 μm and 1.5 μm respectively. The proposed structure has a width of 3 μm but constricts to 1.5 μm at the cross section. By applying

an equal amount of current across the Hall bar, the proposed structure generates a  $H_0$  which is larger than the conventional Hall cross structures with a width of 3 μm and 1.5 μm by 65% and 10% respectively. The larger  $H_0$  enables DWs to be injected with a lower applied current density ( $J_{input}$ ).

Apart from DW injection, the Hall cross structure is also used for Hall resistance ( $R_H$ ) measurements to demonstrate the electric field modulation on the effective anisotropy energy ( $K_{eff}$ ) of the material. Fig. 3(a) shows the normalized  $R_H$  dependence on the out-of-plane magnetic field ( $H_z$ ) with an applied electric field of  $\pm 250$  MV/m. The result demonstrates that the coercivity ( $H_c$ ) of the material can be modulated with electric field control. The reduction of  $H_c$  with an applied electric field of +250 MV/m implies that a smaller Oersted field is required to switch the magnetization. The  $K_{eff}$  of the material can be extracted from the normalized  $R_H$  measurement with an in-plane magnetic field. The normalized  $R_H$  measurement is shown in Fig. 3(b), where the longitudinal magnetic field ( $H_x$ ), is smaller than the  $H_k$  of the device. The inset in the figure shows the vibrating sample magnetometry measurements of the thin film as deposited to obtain the magnetic saturation ( $M_s$ ) of the material.

The normalized  $R_H$  measurement can be modelled to be written as follows, [28,29]

$$R_H^n = \frac{1}{2} \Delta R_H^n \cos(\theta) \tag{1}$$

where  $R_H^n$  is the normalized Hall resistance and  $\Delta R_H^n$  is the maximum resistance change between the up magnetization and down

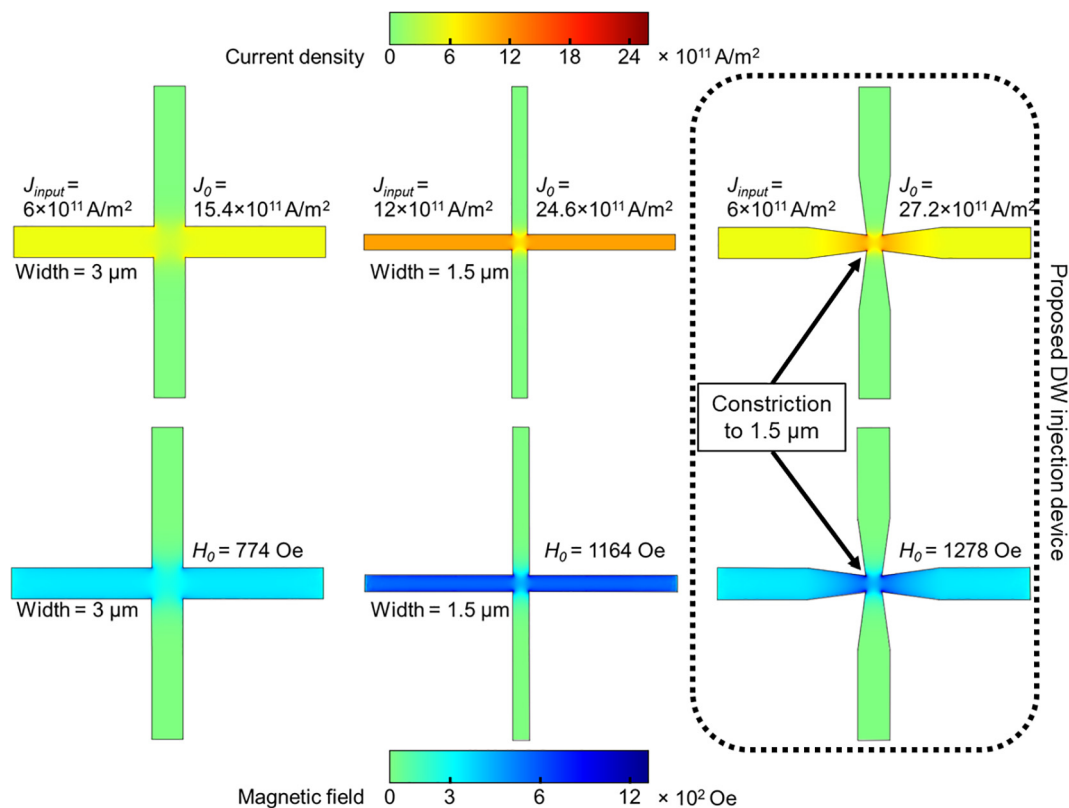


Fig. 2. Current density and Oersted field mapped on to the various Hall cross structure. The  $J_{input}$  in the middle Hall crosses of 1.5  $\mu$ m is twice of the  $J_{input}$  from the other Hall crosses to ensure that the total current (A) in the Hall cross structure is kept constant.

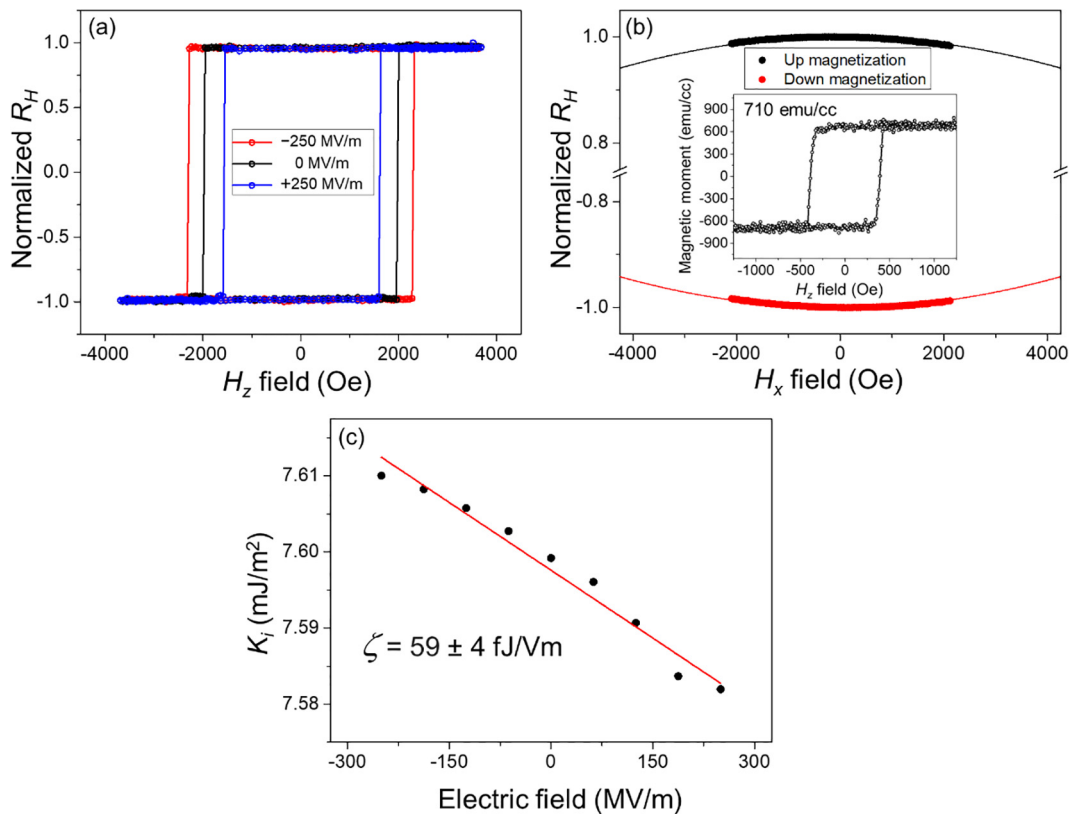


Fig. 3. Normalized  $R_H$  measurement of the Hall cross device with (a) out-of-plane magnetic field and (b) in-plane magnetic field. The lines show the fitting using Eq. (3). The inset shows the results of the thin film measurement using vibrating sample magnetometry to obtain the magnetic saturation of the material. (c)  $K_i$  dependence on applied electric field. The line shows the linear fit, where the obtained gradient of  $59 \pm 4$  fJ/Vm is the VCMA coefficient.

magnetization state of the  $R_H^n$ , hence the value of  $\Delta R_H^n = 2$ .

By utilising the Maclaurin expansion and excluding high order terms, Eq. (1) can be rewritten to be,

$$R_H^n = 1 - \frac{1}{2}\theta^2 = 1 - \frac{H_x^2}{2H_k^2} \quad (2)$$

The value of  $H_k$  can be obtained from a parabolic fitting given by,

$$R_H^n = aH_x^2 \pm 1 \quad (3)$$

where  $\pm$  refers to the up and down magnetization state. Therefore, the  $H_k$  of the material can be found with the following equation,

$$H_k = \pm \sqrt{\frac{1}{2a}} \quad (4)$$

where  $a$  is the parameter from the parabolic fitting.

The effective anisotropy of the material can be obtained with the equation,  $K_{eff} = \frac{1}{2}M_s H_k$ , where  $K_{eff}$  refers to the effective anisotropy energy and  $M_s$  refers to the magnetic saturation of the material.

Assuming the change in interfacial anisotropy ( $K_i$ ) to be the dominant cause of the anisotropy modulation. The  $K_{eff}$  of the device can be modelled to be as follows,

$$K_{eff} = K_{anis} - \frac{\mu_0 M_s^2}{2} = \frac{K_i}{t} - \frac{\mu_0 M_s^2}{2} \quad (5)$$

where  $K_i$  refers to the interfacial anisotropy,  $t$  is the thickness of the magnetic material, and  $\mu_0$  refers to the permeability of free space. Therefore, the  $K_i$  dependence on electric field can be obtained from the gradient of the linear fitting in Fig. 3(c), giving the voltage controlled magnetic anisotropy coefficient,  $\zeta$  to be  $59 \pm 4$  fJ/Vm.

Electrical current pulse of 50 ns is applied through the Hall cross to inject the DWs and the presence of the DWs can be detected from both electrical measurement and Kerr microscopy results. Fig. 4 shows the  $R_H^n$  results after a current pulse of various current density is applied across the Hall cross. A saturation magnetic field was used to remove any DWs before the current pulse was applied. Partial  $H_z$  field sweeps were carried out to detect the switching field of the device. The  $R_H^n$  results show two distinct switching fields at  $\sim 300$  Oe and  $\sim 1500$  Oe. The lower switching field indicates that a domain is formed in the Hall cross, whereby the existing domain expands at  $\sim 300$  Oe, leading to the complete magnetization reversal of the Hall cross.

Although the applied current pulses with current density of  $4.2 \times 10^{11}$  A/m<sup>2</sup> and  $4.7 \times 10^{11}$  A/m<sup>2</sup> in Fig. 4 both indicate the presences of reversed domains, further characterization using the

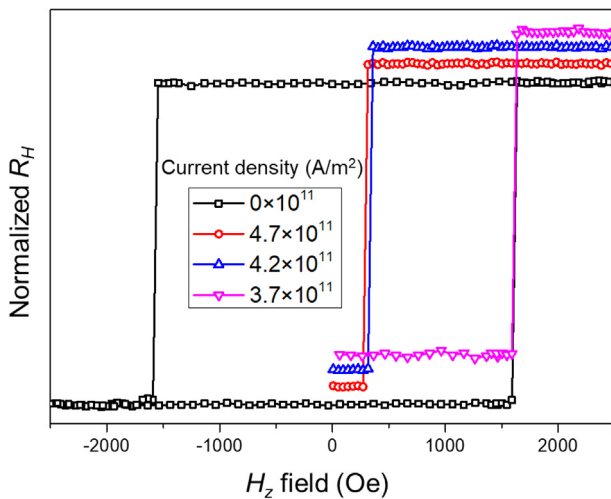


Fig. 4. Electric measurement for domain detection on the Hall cross device. The results have a y offset for visual clarity. The electric measurement displays similar results for full and partial DW injection at current density of  $4.7 \times 10^{11}$  A/m<sup>2</sup> and  $4.2 \times 10^{11}$  A/m<sup>2</sup> respectively.

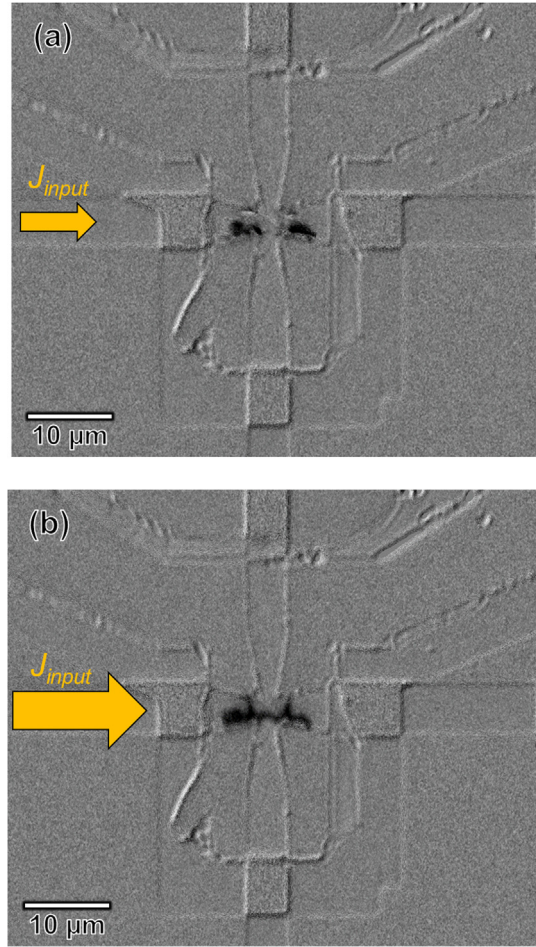
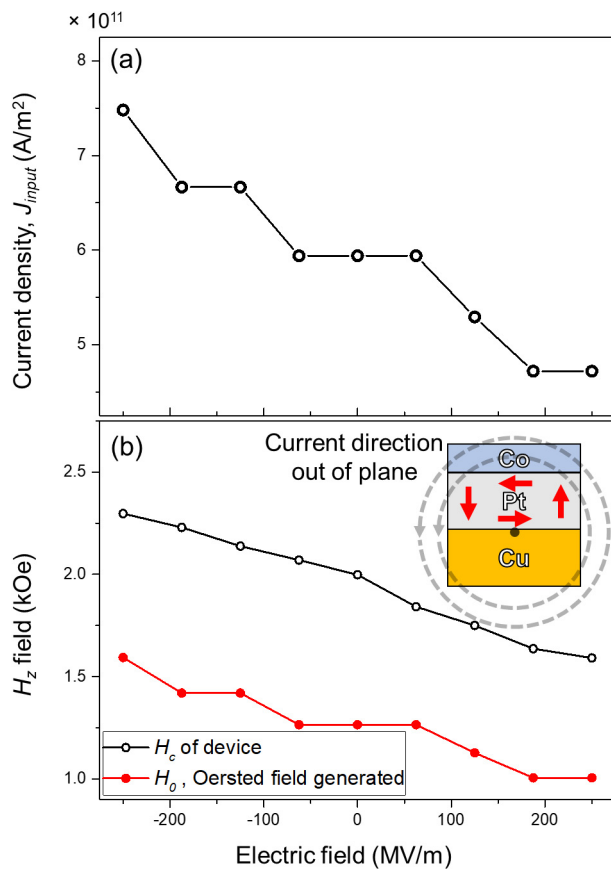


Fig. 5. Kerr images obtained after a current pulse is applied across the Hall cross device (right to left) illustrating (a) a partially formed domain with a  $J_{input}$  of  $4.2 \times 10^{11}$  A/m and (b) a fully formed domain with a larger  $J_{input}$  of  $4.7 \times 10^{11}$  A/m.

MagVision Kerr microscopy system reveals that the DW injection process can be incomplete. The partially injected DWs do not go across the width of the magnetic wire as shown in the Kerr image found in Fig. 5(a). These partially formed DWs can propagate with a magnetic field lower than the  $H_c$  of the Hall cross device just like fully formed DWs that stretch across the width of the wire. Hence, the electrical measurements shown in Fig. 4 was only used as a reference to substantiate the DWs injected observed using Kerr microscopy. In this study, DWs are only considered to be successfully injected when visual inspection of the Kerr images shows that the DWs are stretched across the entire width of the wire as shown in Fig. 5(b).

Electric field was applied onto the Hall cross during the injection current pulse. When a positive electric field is applied, the anisotropy of the device decreases, enabling DWs to be injected with a lower  $J_{input}$ . The opposite is also true when a negative electric field is applied, requiring a higher  $J_{input}$  to inject DWs. The relationship between the required  $J_{input}$  to inject DWs and the applied electric field is shown in Fig. 6(a). The application of a +250 MV/m electric field results in a  $\sim 20\%$  decrease in the required  $J_{input}$  for injection of DWs. The change in the required  $J_{input}$  demonstrates that electric field control has lowered the energy requirement for DW injection.

In Fig. 6(b), the  $H_c$  modulation of the material by the electric field is compared with the simulated Oersted field generated at the corners of the Hall cross structure,  $H_0$ . The difference in the  $H_0$  and the  $H_c$  of the material suggests that there are other effects contributing to the injection of DWs. One such effect could be Joule heating, where the heat



**Fig. 6.** (a) The dependence of the required  $J_{input}$  to inject a fully formed domain across the device at various applied electric field. (b) Comparison of the  $H_0$  generated by the  $J_{input}$  and the  $H_c$  of the material. The inset shows the direction of the Oersted field and the spin current in the Pt layer with the current running out of the current sectional plane. The dotted arrows represent the Oersted field and the red arrows represent the polarized spin current due to spin Hall effect. (For interpretation of the references to colour in this figure legend, the reader is referred to the web version of this article.)

energy lowers the thermal activation threshold for magnetization switching [9,30]. Additionally, unlike the conventional technique where the current goes through a stripline, the current applied through the Hall bar is passing through Hall cross device itself, potentially inducing spin-torque effects. Spin-orbit torque (SOT) has been measured in the stack structure of Pt/Co/Pt [26,27], which is also the stack structure used in this work [31,32]. The thicker Pt layer below the Co layer contributes a larger spin-orbit torque than the top Pt layer due to spin Hall effect (SHE). This allows the overall spin-orbit torque to assist in the local magnetization switching [33,34]. The inset of Fig. 6(b) illustrates how the SHE can assist the local magnetization switching process. During the current injection, spin accumulation occurs at the boundaries of the Pt layer due to SHE. The accumulated spins at the Pt/Co interface applies a torque to the magnetization in the same direction as the Oersted field lines, possibility resulting in a spin orbit torque assisted magnetization switching during the injection of DWs.

In conclusion, a unique DW injection technique assisted by electric field control was demonstrated to lower the required  $J_{input}$  for DW injection in PMA magnetic wires. The geometrically constrained Hall cross structure enables a larger current density at the domain injection region. This gives rise to a local Oersted field, Joule heating and spin-torque effects which contribute towards the local magnetization switching. These effects all arise from the  $J_{input}$  applied across the Hall cross device, and the  $J_{input}$  can be reduced by electric field control. The reduction in the required  $J_{input}$  for DW injection by up to  $\sim 20\%$  using

electric field control would enable a more energy efficient DW injection method for device applications.

## Acknowledgements

The work was supported by the Singapore National Research Foundation, Prime Minister's Office under a Competitive Research Programme (Non-volatile Magnetic Logic and Memory Integrated Circuit Devices, NRF-CRP9-2011-01), and an Industry-IHL Partnership Program (NRF2015-IIP001-001). The supports from a RIE2020 ASTAR AME IAF-ICP Grant (No. I1801E0030) and an ASTAR AME Programmatic Grant (No. A1687b0033) is also acknowledged. WSL is a member of the Singapore Spintronics Consortium (SG-SPIN).

## Appendix A. Supplementary data

Supplementary data to this article can be found online at <https://doi.org/10.1016/j.jmmm.2019.04.069>.

## References

- [1] D. Chiba, G. Yamada, T. Koyama, K. Ueda, H. Tanigawa, S. Fukami, T. Suzuki, N. Ohshima, N. Ishiwata, Y. Nakatani, Control of multiple magnetic domain walls by current in a Co/Ni nano-wire, *Appl. Phys. Exp.* 3 (7) (2010) 073004.
- [2] S. Parkin, S.-H. Yang, Memory on the racetrack, *Nat. Nanotechnol.* 10 (3) (2015) 195.
- [3] S.S. Parkin, M. Hayashi, L. Thomas, Magnetic domain-wall racetrack memory, *Science* 320 (5873) (2008) 190–194.
- [4] Y. Zhang, C. Zhang, J.-O. Klein, D. Ravelosona, G. Sun, W. Zhao, Perspectives of racetrack memory based on current-induced domain wall motion: From device to system, *IEEE* (2015).
- [5] C. Chappert, A. Fert, F.N. Van Dau, The emergence of spin electronics in data storage, *Nanosci. Technol. A Collect. Rev. Nat. J.* (2010) 147–157.
- [6] S. Ikeda, K. Miura, H. Yamamoto, K. Mizunuma, H. Gan, M. Endo, S. Kanai, J. Hayakawa, F. Matsukura, H. Ohno, A perpendicular-anisotropy CoFeB–MgO magnetic tunnel junction, *Nat. Mater.* 9 (9) (2010) 721.
- [7] S.H. Charap, P.-L. Lu, Y. He, Thermal stability of recorded information at high densities, *IEEE Trans. Magn.* 33 (1) (1997) 978–983.
- [8] D. Weller, A. Moser, L. Folks, M.E. Best, W. Lee, M.F. Toney, M. Schwickert, J.-U. Thiele, M.F. Doerner, High K/sub u/materials approach to 100 Gbits/in/sup 2, *IEEE Trans. Magn.* 36 (1) (2000) 10–15.
- [9] S. Zhang, W. Gan, J. Kwon, F. Luo, G. Lim, J. Wang, W. Lew, Highly efficient domain walls injection in perpendicular magnetic anisotropy nanowire, *Sci. Rep.* (2016) 6.
- [10] S. Fukami, M. Yamanouchi, S. Ikeda, H. Ohno, Depinning probability of a magnetic domain wall in nanowires by spin-polarized currents, *Nat. Commun.* 4 (2013) 2293.
- [11] S. Emori, U. Bauer, S.-M. Ahn, E. Martinez, G.S. Beach, Current-driven dynamics of chiral ferromagnetic domain walls, *Nat. Mater.* 12 (7) (2013) 611.
- [12] K. Ueda, K.-J. Kim, T. Taniguchi, T. Tono, T. Moriyama, T. Ono, In-plane field-driven crossover in the spin-torque mechanism acting on magnetic domain walls in Co/Ni, *Phys. Rev. B* 91 (6) (2015) 060405.
- [13] D.A. Allwood, G. Xiong, C. Faulkner, D. Atkinson, D. Petit, R. Cowburn, Magnetic domain-wall logic, *Science* 309 (5741) (2005) 1688–1692.
- [14] J. Kwon, S. Goolaup, F. Tan, C.H. Chang, K. Roy, W.S. Lew, Cyclic resistance change in perpendicularly magnetized Co/Ni nanowire induced by alternating current pulse injection, *Curr. Appl. Phys.* 17 (1) (2017) 98–102.
- [15] P. Sethi, S. Krishnia, W. Gan, F. Kholid, F. Tan, R. Maddu, W. Lew, Bi-directional high speed domain wall motion in perpendicular magnetic anisotropy Co/Pt double stack structures, *Sci. Rep.* (2017) 7.
- [16] T. Koyama, K. Ueda, K.-J. Kim, Y. Yoshimura, D. Chiba, K. Yamada, J.-P. Jamet, A. Mougin, A. Thiaville, S. Mizukami, Current-induced magnetic domain wall motion below intrinsic threshold triggered by Walker breakdown, *Nat. Nanotechnol.* 7 (10) (2012) 635.
- [17] T. Koyama, D. Chiba, K. Ueda, K. Kondou, H. Tanigawa, S. Fukami, T. Suzuki, N. Ohshima, N. Ishiwata, Y. Nakatani, Observation of the intrinsic pinning of a magnetic domain wall in a ferromagnetic nanowire, *Nat. Mater.* 10 (3) (2011) 194.
- [18] Q. Wong, W. Gan, F. Luo, G. Lim, C. Ang, F. Tan, W. Law, W. Lew, In situ Kerr and harmonic measurement in determining current-induced effective fields in MgO/CoFeB/Ta, *J. Phys. D Appl. Phys.* 51 (11) (2018) 115004.
- [19] T. Jin, F. Tan, W.C. Law, W. Gan, I. Soldatov, R. Schäfer, C. Ma, X. Liu, W.S. Lew, S. Piramanayagam, Nanoscale modification of magnetic properties for effective domain wall pinning, *J. Magnet. Magn. Mater.* (2018).
- [20] F. Tan, G.J. Lim, W.C. Law, F. Luo, H. Liu, F. Poh, D. Shum, W. Lew, Electric field control on gated Pt/Co/SiO<sub>2</sub> heterostructure with insulating polymer, *J. Phys. D: Appl. Phys.* (2018).
- [21] E. Martinez, S. Emori, G.S. Beach, Current-driven domain wall motion along high perpendicular anisotropy multilayers: The role of the Rashba field, the spin Hall effect, and the Dzyaloshinskii-Moriya interaction, *Appl. Phys. Lett.* 103 (7) (2013) 072406.

- [22] U. Bauer, S. Emori, G.S. Beach, Electric field control of domain wall propagation in Pt/Co/GdOx films, *Appl. Phys. Lett.* 100 (19) (2012) 192408.
- [23] U. Bauer, L. Yao, A.J. Tan, P. Agrawal, S. Emori, H.L. Tuller, S. Van Dijken, G.S. Beach, Magneto-ionic control of interfacial magnetism, *Nat. Mater.* 14 (2) (2015) 174.
- [24] K. Yamada, H. Kakizakai, K. Shimamura, M. Kawaguchi, S. Fukami, N. Ishiwata, D. Chiba, T. Ono, Electric field modulation of magnetic anisotropy in MgO/Co/Pt structure, *Appl. Phys. Exp.* 6 (7) (2013) 073004.
- [25] Y. Hibino, T. Koyama, A. Obinata, K. Miwa, S. Ono, D. Chiba, Electric field modulation of magnetic anisotropy in perpendicularly magnetized Pt/Co structure with a Pd top layer, *Appl. Phys. Exp.* 8 (11) (2015) 113002.
- [26] D. Chiba, M. Kawaguchi, S. Fukami, N. Ishiwata, K. Shimamura, K. Kobayashi, T. Ono, Electric-field control of magnetic domain-wall velocity in ultrathin cobalt with perpendicular magnetization, *Nat. Commun.* 3 (2012) 888.
- [27] F. Ando, H. Kakizakai, T. Koyama, K. Yamada, M. Kawaguchi, S. Kim, K.-J. Kim, T. Moriyama, D. Chiba, T. Ono, Modulation of the magnetic domain size induced by an electric field, *Appl. Phys. Lett.* 109 (2) (2016) 022401.
- [28] Y.-C. Lau, P. Sheng, S. Mitani, D. Chiba, M. Hayashi, Electric field modulation of the non-linear areal magnetic anisotropy energy, *Appl. Phys. Lett.* 110 (2) (2017) 022405.
- [29] H.-R. Lee, K. Lee, J. Cho, Y.-H. Choi, C.-Y. You, M.-H. Jung, F. Bonell, Y. Shiota, S. Miwa, Y. Suzuki, Spin-orbit torque in a bulk perpendicular magnetic anisotropy Pd/FePd/MgO system, *Sci. Rep.* 4 (2014) 6548.
- [30] R.H. Koch, G. Grinstein, G. Keefe, Y. Lu, P. Trouilloud, W. Gallagher, S. Parkin, Thermally assisted magnetization reversal in submicron-sized magnetic thin films, *Phys. Rev. Lett.* 84 (23) (2000) 5419.
- [31] C. Hin Sim, J. Cheng Huang, M. Tran, K. Eason, Asymmetry in effective fields of spin-orbit torques in Pt/Co/Pt stacks, *Appl. Phys. Lett.* 104 (1) (2014) 012408.
- [32] S. Li, G. Lim, W. Gan, W. Law, F. Tan, W. Lew, Tuning the spin-orbit torque effective fields by varying Pt insertion layer thickness in perpendicularly magnetized Pt/Co/Pt (t)/Ta structures, *J. Magnet. Magnet. Mater.* 473 (2019) 394–398.
- [33] S.V. Aradhya, G.E. Rowlands, J. Oh, D.C. Ralph, R.A. Buhrman, Nanosecond-timescale low energy switching of in-plane magnetic tunnel junctions through dynamic oersted-field-assisted spin Hall effect, *Nano Lett.* 16 (10) (2016) 5987–5992.
- [34] T. Skinner, M. Wang, A. Hindmarch, A. Rushforth, A. Irvine, D. Heiss, H. Kurebayashi, A. Ferguson, Spin-orbit torque opposing the Oersted torque in ultrathin Co/Pt bilayers, *Appl. Phys. Lett.* 104 (6) (2014) 062401.